



## **Tungsten-Copper Composites for Arcing Contact Applications in High Voltage Circuit Breakers**

**MAGDALENA VALENTINA LUNGU<sup>1\*</sup>, DELIA PATROI<sup>1</sup>, VIRGIL MARINESCU<sup>1</sup>,  
SORINA MITREA<sup>1</sup>, IOANA ION<sup>1</sup>, MIHAI MARIN<sup>1</sup> and PETRISOR GODEANU<sup>2</sup>**

<sup>1</sup>National Institute for Research and Development in Electrical Engineering  
ICPE-CA, 313 Splaiul Unirii Street, 030138 Bucharest, Romania.

<sup>2</sup>MAIRA MONTAJ SRL, 166 Stirbei Voda Street, 010121 Bucharest, Romania.

### **Abstract**

The study presents the research findings on electrical contact materials based on tungsten-copper (W-Cu) composites containing  $72 \pm 3$  wt.% W, rest Cu, and up to 1.5 wt.% Ni. Cylindrical sintered parts with  $57 \pm 0.5$  mm in diameter and  $12 \pm 0.5$  mm in height were manufactured by pressing, sintering, and liquid infiltration route, then were mechanically polished and processed as complex shape protection rings used as arcing contacts in high voltage circuit breakers (HVCBs). The surface elemental composition of the sintered parts was determined by wavelength dispersive X-ray fluorescence spectrometry. The density was determined by hydrostatic weighing in ethanol. The arithmetic mean surface roughness was measured by contact profilometry. The microstructure was studied by scanning electron microscopy. The electrical conductivity was measured by eddy current method. The thermal diffusivity and specific heat were determined by laser flash analysis. Instrumented indentation testing and two computational methods (Oliver & Pharr, and Martens hardness) were employed to study the mechanical properties under quadratic loading and continuous multi cycle (CMC) indentation mode. The functional behavior of the arcing contacts was assessed in terms of static and dynamic contact resistance in operation in minimum oil HVCBs of 110 kV. The properties investigation revealed highly dense contact parts with homogeneous microstructure, Vickers hardness of 260-374, elastic modulus of 185-311 GPa, as well as good electrical and thermal conductivity. The arcing contacts proved a good functional behavior. in service, too. The results endorse the developed sintered contact materials for implementation in practical applications.



### **Article History**

Received: 20 June 2020

Accepted: 22 July 2020

### **Keywords:**

Arcing Contacts;  
High Voltage Circuit  
Breakers;  
Protection Rings;  
Sintered Contact  
Materials;  
Tungsten-Copper.

**CONTACT** Magdalena Valentina Lungu ✉ [magdalena.lungu@icpe-ca.ro](mailto:magdalena.lungu@icpe-ca.ro) 📍 National Institute for Research and Development in Electrical Engineering ICPE-CA, Metallic, Composite and Polymeric Materials Department, 313 Splaiul Unirii Street, 030138 Bucharest, Romania.



© 2020 The Author(s). Published by Oriental Scientific Publishing Company

This is an Open Access article licensed under a Creative Commons Attribution-NonCommercial-ShareAlike 4.0 International License  
Doi: <http://dx.doi.org/10.13005/msri/170304>

## Introduction

W-Cu electrical contact materials are widely used as make/break and arcing contacts for equipping low, medium and high voltage switching devices such as power switches and circuit breakers. They operate in various arc quenching media, from which most common ones are vacuum, mineral oil and sulphur hexafluoride (SF<sub>6</sub>) gas.<sup>1-8</sup>

W-Cu contacts can be manufactured only by powder metallurgy (PM) techniques. The reason is related to the fact that W and Cu are dissimilar engineering materials with large differences between their properties. Moreover, these materials exhibit a relatively poor wettability between solid W phase and liquid Cu and mutual insolubility due to insignificant solubility ( $< 10^{-3}$  at.% Cu).<sup>9, 10</sup>

It is known that common PM techniques include powder processing and consolidation by pressing and sintering followed by repressing or infiltration. On the other hand, unconventional PM techniques involve hot or cold isostatic pressing, spark plasma sintering, and microwave sintering.<sup>1-17</sup> The advantages of PM techniques consist in obtaining advanced composite materials by combining and preserving properties of individual components. In case of W-Cu contact materials of great importance are outstanding electrical and thermal properties of Cu metal, as well as excellent mechanical properties of refractory and heavy W metal.<sup>1</sup>

By comparing the representative properties of W and Cu at 20°C (293 K) can be noticed that Cu has the electrical conductivity ( $5.98 \times 10^7$  S/m) and thermal conductivity (403 W/(mK)) of about 3.3 times, and 2.3 times, respectively, greater than the ones of W ( $1.82 \times 10^7$  S/m, and 174 W/(mK), respectively). The density of W ( $19.3 \text{ g/cm}^3$ ) is about 2.2 times greater than the density of Cu ( $8.96 \text{ g/cm}^3$ ), while the melting temperature of W (3410°C) is about 3.2 times greater than the one of Cu (1083°C). Therefore, choosing the right W-Cu composition and PM consolidation technique leads to obtaining W-Cu electrical contacts that can withstand the difficult and hard regime conditions during make/break operations in a real environment in service.

Most of the literature studies report the development of W-Cu electrical contacts starting from micro

or nano crystalline composite powders that are consolidated by various PM techniques in small size contact parts having no more than 20 mm in diameter.<sup>18-25</sup> Generally, the developed contact parts were investigated in terms of microstructure, along with physical, chemical, electrical, thermal, and mechanical properties. The functional behavior of W-Cu electrical contacts in operation in power switching devices is presented and discussed in a few reports<sup>18-25</sup> even it is decisive in qualifying W-Cu electrical contacts for implementation in practical applications.

The starting powders, synthesis method for achieving W-Cu composites, and process parameters for composite powder consolidation can greatly influence the properties of W-Cu arcing contacts. Therefore, the researches in this field are of considerable interest to the producers and industrial end-users to develop W-Cu arcing contacts with superior properties and cost-saving prices to increase the lifetime of switching devices they equip.

In these research works, the main objective was to develop large size and reliable W-Cu electrical contact materials by employing a pressing, sintering, and liquid infiltration route, followed by mechanical polishing and processing to manufacture complex shape protection rings for arcing contact applications in HVCBs. The sintered contact materials were studied in terms of microstructure, surface elemental composition, density, relative density, surface roughness, electrical conductivity, electrical resistivity, thermal diffusivity, specific heat, thermal conductivity, hardness, elastic modulus, and creep. The developed contact materials exhibited properties that are in agreement with those recommended by the standard ASTM B702-93(2019) that is the standard specification for W-Cu electrical contact materials. The functional behavior of the realized arcing contacts was proved in real operating conditions by measuring the static and dynamic contact resistance in minimum oil HVCBs of 110 kV. The measured contact resistance values were in the maximum admissible limit of 0.2 mΩ required by the standard IEC 62271-100 for HVCBs. The obtained results endorse the elaborated sintered contact materials based on W-Cu composites for utilization as arcing contacts in electric power applications, specifically in minimum oil HVCBs.

### Experimental

The elemental powders used in this study consisted of commercially fine and pure powders of W (> 99.9 %, Fisher particle size of 4.2  $\mu\text{m}$ , Scott density of 3.55  $\text{g/cm}^3$ , Global Tungsten & Powders (GTP) spol. s.r.o., Czech Republic), electrolytic Cu (> 99.9 %, maximum particle size of 63  $\mu\text{m}$ , apparent density of 1.6  $\text{g/cm}^3$ , GGP Metal-powder AG, Germany), and Ni (99.7 %, maximum particle size of 50  $\mu\text{m}$ , Merck, Germany).

Ni doped and undoped W based porous skeletons with  $57 \pm 0.5$  mm in diameter and  $12 \pm 0.5$  mm in height were achieved by pressing at a certain porosity the composite powder mixtures containing specific amounts of elemental powders that were previously blended and homogenized with stainless steel balls in a Turbula shaker mixer as we described elsewhere.<sup>6</sup>

The designed composition of the final contact materials was W-Cu-Ni 75-24-1 (theoretical density of 14.977  $\text{g/cm}^3$ ) and W-Cu 75-25 (theoretical density of 14.979  $\text{g/cm}^3$ ).

W-Cu based cylindrical semi-finished parts with  $57 \pm 0.5$  mm in diameter and  $12 \pm 0.5$  mm in height were manufactured in similar conditions shown by us in another study for obtaining cylindrical semi-finished parts with  $50 \pm 0.5$  mm in diameter and  $6 \pm 0.5$  mm in height.<sup>6</sup>

The obtained W-Cu cylindrical semi-finished parts were mechanically polished and processed as complex shape protection rings for utilization as arcing contacts in HVCBs of 110 kV. Some analyses required the using of small size rectangular ( $5 \pm 0.1$  mm x  $2.9 \pm 0.1$  mm) and cylindrical ( $\varnothing 12.6 \pm 0.1$  mm x  $2.9 \pm 0.1$  mm) samples cut from the central part of the large size semi-finished parts.

The surface elemental composition was assessed on the contact surface of the developed W-Cu semi-finished parts using a Bruker S8 Tiger 1K wavelength dispersive X-ray fluorescence (WDXRF) spectrometer.

The density was determined by hydrostatic weighing of the sintered samples ( $\varnothing 12.6 \pm 0.1$  mm x  $2.9 \pm 0.1$  mm) employing a Kern AEJ analytical balance and

ethanol as a liquid medium. The mean values of three measurements performed at 23°C (temperature of ethanol) are reported along with their relative density to theoretical density and porosity.

The arithmetic mean surface roughness ( $R_a$ ) of the sintered parts was measured at room temperature (RT) using a Surtronic S25 Taylor & Hobson contact profilometer, an evaluation length of 4 mm, a cut-off of 0.8, and a Gaussian filter.

The microstructure of the samples ( $5 \pm 0.1$  mm x  $2.9 \pm 0.1$  mm) embedded in resin and mirror surface finished with fine alumina was studied by scanning electron microscopy (SEM) using an Auriga CrossBeam workstation equipped with a secondary electron secondary ion (SESI) detector working at 5 kV DC acceleration voltage in vacuum.

The mean values of electrical conductivity of the sintered parts measured in triplicate at RT by eddy current method using a Sigmascope EX8 device are reported.

The thermal diffusivity and specific heat of the sintered samples ( $\varnothing 12.6 \pm 0.1$  mm x  $2.9 \pm 0.1$  mm) were measured at 25°C by laser flash analysis (LFA) using a Netzsch LFA 447 NanoFlash apparatus, and an Inconel 600 reference, as we detailed elsewhere.<sup>6</sup>

The mechanical properties, namely indentation hardness ( $H_{IT}$ ), Vickers hardness ( $HV_{IT}$ ), indentation elastic modulus ( $E_{IT}$ ), indentation creep ( $C_{IT}$ ) and Martens hardness (HM) were measured at RT by instrumented indentation testing (IIT) and Oliver & Pharr method, and Martens hardness method, respectively.<sup>6, 26, 27</sup> A CSM Instruments Micro-Combi Tester (MCT<sup>2</sup>) equipped with a nanoindentation hardness tester (NHT) and a diamond Berkovich indenter were used. The IIT measurements were performed on the contact surface of the developed W-Cu semi-finished parts under quadratic loading and continuous multi cycle (CMC) indentation mode, as follows: 20 cycles, maximum load in the first cycle of 20 mN, unloading to 20% of the maximum load in the given cycle, maximum load in the last cycle of 200 mN, time to maximum load of 30 s, time to unload of 30 s, pause of 10 s, pause between cycles of 10 s, approach speed of the indenter of 2000 nm/min, and acquisition rate of 10 Hz.

The functional tests of the developed W-Cu arcing contacts (complex shape protection rings) were performed in minimum oil HVCBs of 110 kV, using an ISA CBA 1000 circuit breakers analyzer. An inhibited transformer oil of PRISTA Trafo-A grade consisting of a naphthenic based mineral oil additized with phenolic based antioxidant was employed as arc quenching medium. The tests comprised the determination of the static ( $R_s$ ) and dynamic contact resistance ( $R_d$ ), according to the standard IEC 62271-100.  $R_s$  was determined by measuring the

resistance at the injected nominal current ( $I_n$ ) of 200 A, after plugging the fixed arcing contact into the tulip contact of the HVCB. For  $R_d$  testing, the times to reach  $R_s$ , as well as the resistance variations on the whole cycle were measured.

### Results and discussion

Fig. 1 shows the aspect of the developed W-Cu electrical contact parts in form of cylindrical shape semi-finished part, and complex shape protection ring.

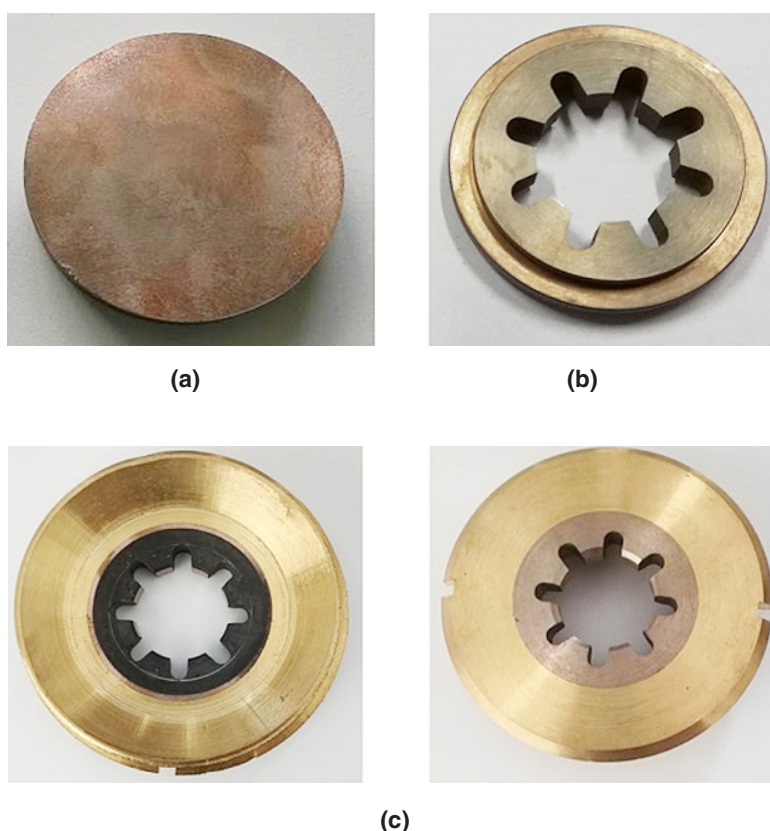


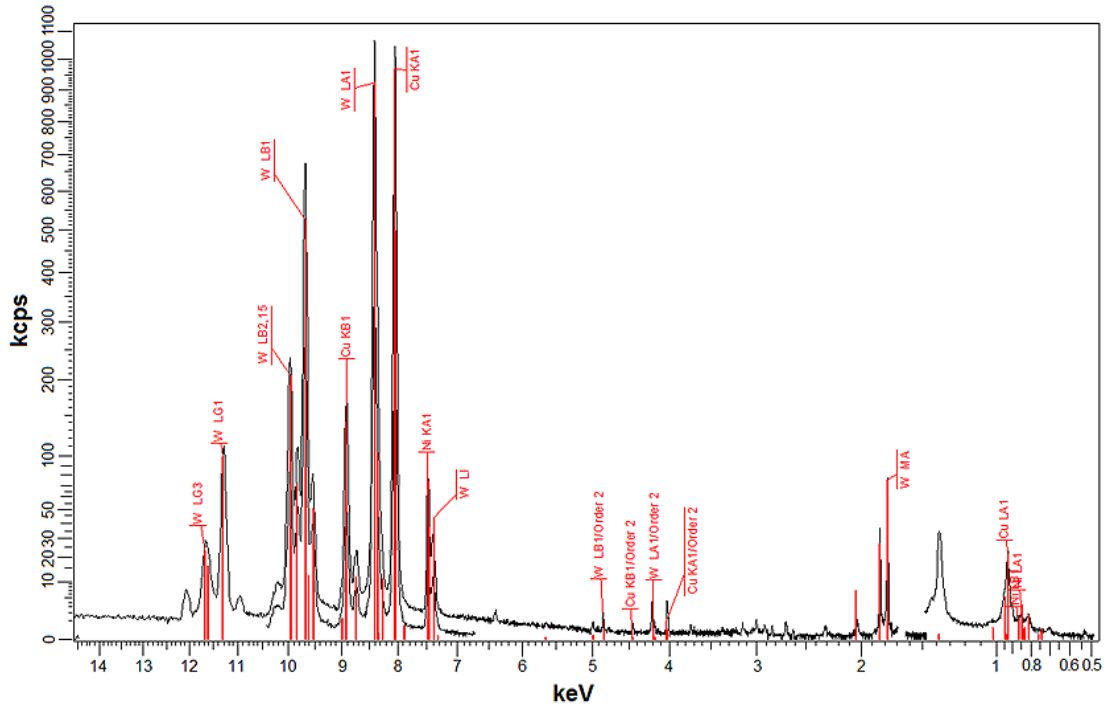
**Fig. 1: Aspect of W-Cu electrical contact parts: (a) cylindrical shape semi-finished part, (b) complex shape protection ring after mechanical processing, (c) protection ring embedded in bronze and prepared for functional testing**

All the sintered samples (Fig. 1) had similar aspect since the small amount of Ni from W-Cu electrical contacts did not influence their color.

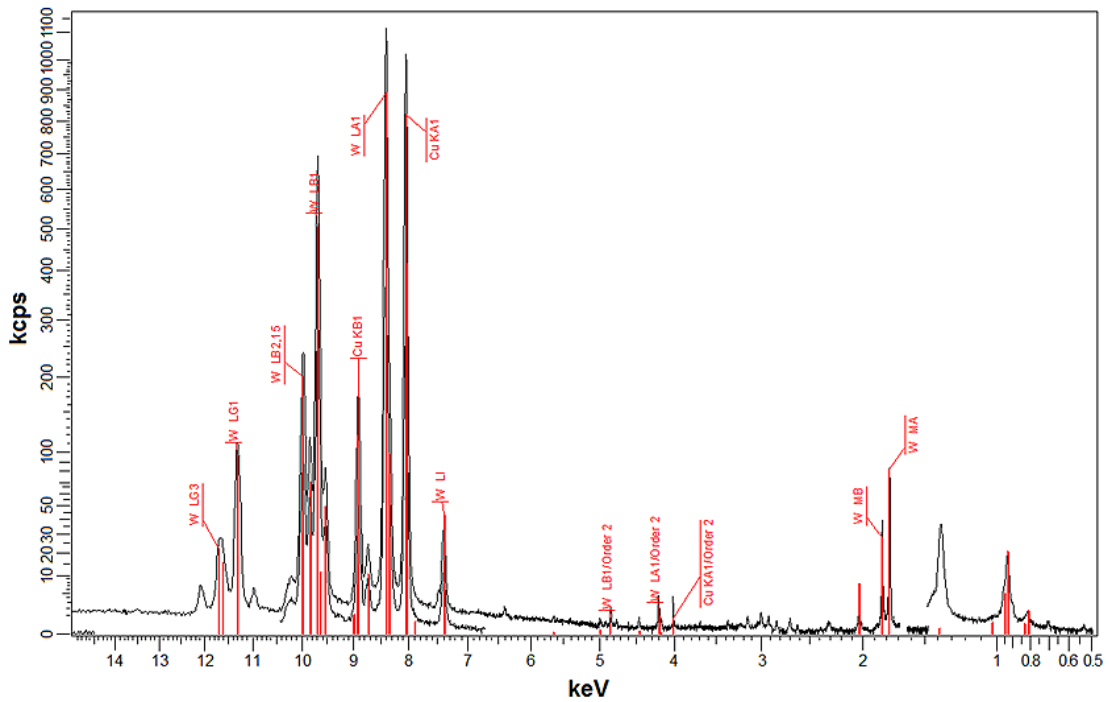
In Table 1 are summarized the results obtained by WDXRF spectrometry for Ni doped and undoped W-Cu contact parts. The most intense spectral line

was W LA1-HR-Tr for W ( $Z = 74$ ), Cu KA1-HR-Tr for Cu ( $Z = 29$ ), and Ni KA1-HR-Tr ( $Z = 28$ ) (Fig. 2).

The unmarked spectral lines (Fig. 2) are specific to the X radiation characteristics to the rhodium (Rh) element used as the anode in the X-ray tube for radiation source.



(a)



(b)

Fig. 2: XRF spectra of (a) Ni doped, and (b) undoped W-Cu electrical contact parts

**Table 1: Elemental composition of Ni doped and undoped W-Cu contact parts determined by WDXRF spectrometry**

Element	Concentration (wt.%)	Most intense spectral line	Net intensity (kcps)	Statistic error (%)	Lower limit of detection (ppm)	Thickness of the analyzed layer ( $\mu\text{m}$ )
<b>Ni doped W-Cu contact part</b>						
W	70.09	W LA1-HR-Tr	1068	0.17	527.9	8.4
Cu	28.46	Cu KA1-HR-Tr	284	0.34	395.5	7.8
Ni	1.45	Ni KA1-HR-Tr	18	1.38	112.2	6.5
<b>Undoped W-Cu contact part</b>						
W	71.94	W LA1-HR-Tr	1110	0.17	515.5	8.5
Cu	28.06	Cu KA1-HR-Tr	278	0.34	411.7	7.6

The elemental composition analysis of the Ni doped W-Cu contact parts revealed a weight content of 70.09 % W, 28.46 % Cu, and 1.45 % Ni, while the undoped W-Cu contact parts exhibited a weight content of 71.94 % W, and 28.06 % Cu. The

composition determined by WDXRF spectrometry is close to the composition designed in the experimental works. High purity of the developed contact materials was confirmed, because other elements besides W, Cu and Ni were not detected.

**Table 2: Mean values  $\pm$  standard deviation (SD) for density, relative density, and porosity of W-Cu sintered materials**

Sintered contact material	Mean exp. density $\pm$ SD ( $\text{g}/\text{cm}^3$ )	Mean relative density $\pm$ SD (%)	Mean porosity $\pm$ SD (%)	Mean volume fraction porosity $\pm$ SD (%)
W-Cu-Ni 75-24-1	13.99 $\pm$ 0.06	93.39 $\pm$ 0.37	6.61 $\pm$ 0.37	11.05 $\pm$ 0.61
W-Cu 75-25	14.14 $\pm$ 0.07	94.42 $\pm$ 0.49	5.58 $\pm$ 0.49	9.33 $\pm$ 0.82

Table 2 shows the mean values and standard deviation (SD) for density, relative density, and porosity of W-Cu sintered materials.

The relative density,  $d_{\text{rel}}$  (%) was calculated with the equation (1):<sup>6</sup>

$$d_{\text{rel}} = (d_{\text{exp}}/d_{\text{th}}) \times 100 \quad \dots(1)$$

The porosity, P (%) was calculated according to the equation (2):<sup>6</sup>

$$P = [(d_{\text{th}} - d_{\text{exp}})/d_{\text{th}}] \times 100 \quad \dots(2)$$

The volume fraction porosity, X (%) was calculated with the equation (3):<sup>12</sup>

$$X = [(d_{\text{th}} - d_{\text{exp}})/d_{\text{Cu}}] \times 100 \quad \dots(3)$$

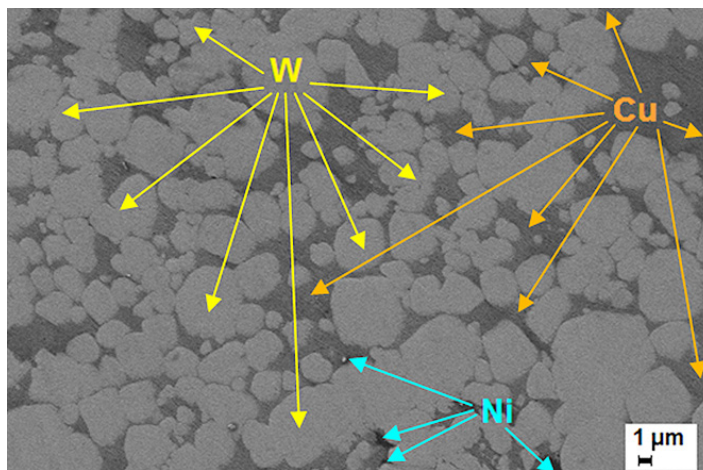
In the above equations,  $d_{\text{th}}$  ( $\text{g}/\text{cm}^3$ ) is the theoretical density of the composite,  $d_{\text{exp}}$  ( $\text{g}/\text{cm}^3$ ) is the experimental density of the sintered composite,  $d_{\text{Cu}}$  is copper density ( $8.96 \text{ g}/\text{cm}^3$ ).

It was revealed the obtaining of dense materials with the density close to their theoretical density, and low porosity (Table 2). W-Cu 75-25 sintered material was

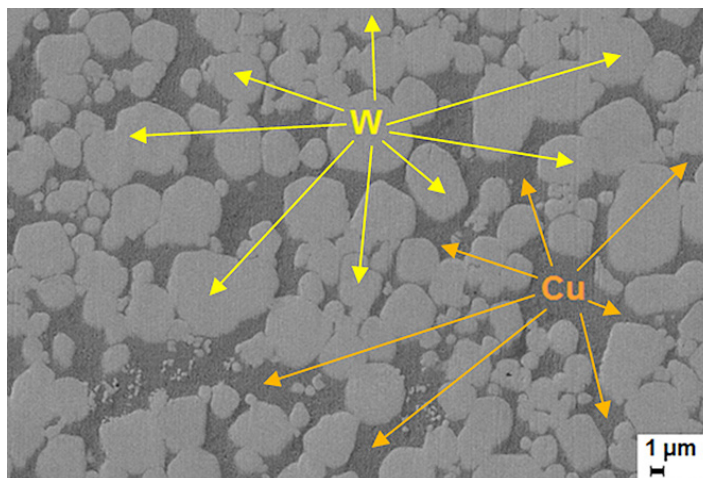
denser than Ni doped W-Cu sintered material. As other literature reports proved, it is very difficult to achieve the full density of W-Cu composite materials by pressing, sintering, and liquid infiltration route due to the mutual insolubility between W and Cu.<sup>9, 10, 29</sup>

The arithmetic mean surface roughness Ra of the sintered parts measured by contact profilometry ranged between 0.10  $\mu\text{m}$  and 0.18  $\mu\text{m}$ . Thus, it was confirmed the achievement of fine surface finishing of the W-Cu sintered parts resulted after the mechanical polishing step.

Fig. 3 depicts the SEM micrographs of the developed W-Cu sintered materials. All composites exhibited a dense microstructure with low porosity that contributes to the accomplishment of high material performance. The presence of W heavy element ( $Z = 74$ ) can be noticed in light gray areas, whereas Cu element ( $Z = 29$ ) can be identified in dark gray areas. These remarks are in concordance with other literature reports.<sup>1, 12, 29</sup>



(a)



(b)

**Fig. 3: SEM micrographs of (a) W-Cu-Ni 75-24-1, and (b) W-Cu 75-25 sintered contact materials (magnification of 5000x, scale bar of 1  $\mu\text{m}$ )**

Ni element used as sintering additive can be identified generally in the small areas with black color. In our study the presence of 1 wt.% of Ni ( $Z = 28$ ) is difficult to be shown in SEM micrographs (Fig. 3) due to a non-homogeneous distribution in W-Cu-Ni 75-24-1 composite.

The morphology of Ni doped and undoped W-Cu sintered materials consisted of irregular shape W particles within the Cu matrix. Both types of composites had approximately homogeneous microstructure with fine W particles and without noticeable pores that is in agreement with the experimental density of the sintered composites.

Above the melting temperature of Cu ( $1083^{\circ}\text{C}$ ), the liquid phase sintering (LPS) occurred. Thus, the dominant mechanism for the densification of W based skeleton compacts is attributed to the rearrangement of W particles due to capillary forces. Besides, W sintering by solid-state diffusion occurs.<sup>12</sup> Ni doping of W-Cu composites led to the improvement of the solid-state sintering of W particles before the liquid phase occurrence. Nevertheless, as Cu melts, Ni

can be dissolved into the liquid phase, so that the solid-state sintering phenomenon is hindered. Also, the solubility of W in the Cu liquid phase is increased, whereas the solid-liquid surface energy is decreased. Besides, Ni contributes to the improvement of the wettability of W combined with melted Cu.<sup>28</sup>

The mean electrical and thermal conductivity values of W-Cu-Ni 75-24-1 sintered contact materials were  $14.3 \pm 1.1 \text{ m}/(\Omega \cdot \text{mm}^2)$ , and  $119.5 \pm 6.4 \text{ W}/(\text{m} \cdot \text{K})$ , respectively, whereas for W-Cu 75-25 sintered materials the values were about double (Table 3, and Table 4). In contrast, the electrical resistivity,  $\rho$  ( $\mu\Omega \cdot \text{cm}$ ) was about double for Ni doped W-Cu sintered material since the electrical resistivity is the inverse of the electrical conductivity. By expressing the electrical conductivity ( $\sigma$ ) in percentages of International Annealed Copper Standard (% IACS) as in the equation (4),<sup>6, 29</sup> it was found that the value of the electrical conductivity is also almost double for the undoped W-Cu sintered material.

$$\sigma = 172.41/\rho \quad \dots(4)$$

**Table 3: Mean values  $\pm$  standard deviation (SD) for electrical conductivity and resistivity of W-Cu sintered contact materials**

Sintered contact material	Mean electrical conductivity $\pm$ SD		Mean electrical resistivity $\pm$ SD
	( $\text{m}/\Omega \cdot \text{mm}^2$ )	(% IACS)	( $\mu\Omega \cdot \text{cm}$ )
W-Cu-Ni 75-24-1	$14.3 \pm 1.1$	$24.6 \pm 1.8$	$7.0 \pm 0.5$
W-Cu 75-25	$29.0 \pm 1.4$	$50.1 \pm 2.5$	$3.5 \pm 0.2$

**Table 4: Mean values  $\pm$  standard deviation (SD) for thermal diffusivity, specific heat and thermal conductivity of W-Cu sintered contact materials**

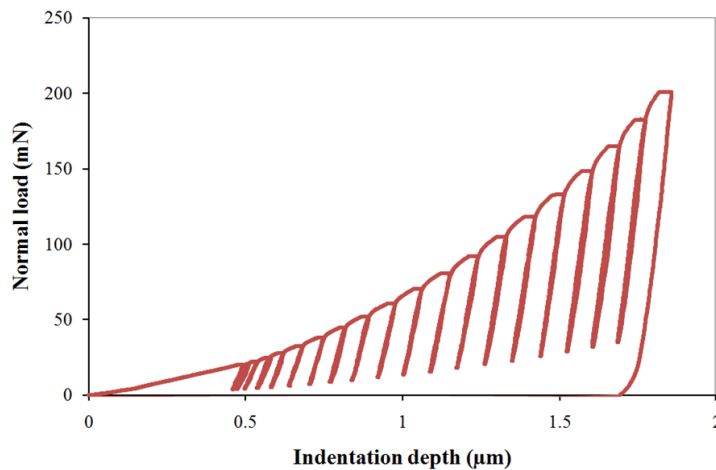
Sintered contact material	Mean thermal diffusivity $\pm$ SD ( $\text{mm}^2/\text{s}$ )	Mean specific heat $\pm$ SD ( $\text{J}/\text{g} \cdot \text{K}$ )	Mean thermal conductivity $\pm$ SD ( $\text{W}/\text{m} \cdot \text{K}$ )
W-Cu-Ni 75-24-1	$44.5 \pm 0.7$	$0.195 \pm 0.004$	$119.5 \pm 6.4$
W-Cu 75-25	$83.5 \pm 0.7$	$0.203 \pm 0.007$	$232.0 \pm 7.1$

W-Cu 75-25 sintered materials yielded superior thermal properties compared with W-Cu-Ni 75-24-1 sintered materials due to the lack of Ni addition. Moreover, the decreased volume fraction of porosity of W-Cu 75-25 sintered materials enhanced both thermal and electrical conductivities in comparison with Ni doped W-Cu sintered materials. These findings are in good accordance with the literature data reported in studies on this class of contact materials.<sup>5, 12, 29-30</sup>

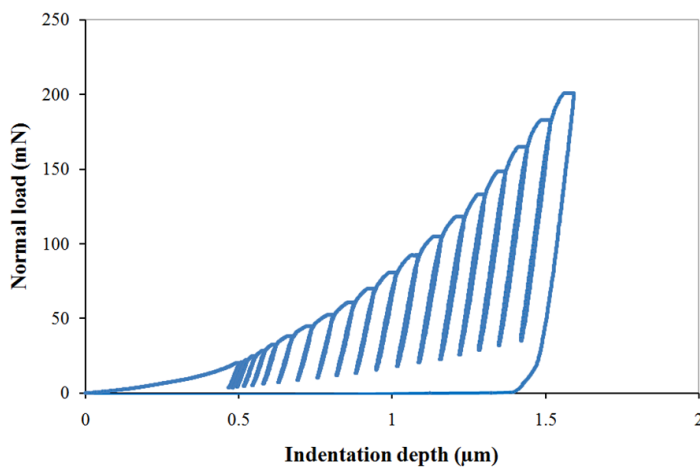
In quadratic loading, the loading ( $F$ ) of the indenter follows the equation (5),<sup>31</sup> shown below:

$$F = k.t^2 \quad \dots(5)$$

where  $k$  represents the loading rate (in mN/min) and  $t$  represents the indentation time (in min).



(a)



(b)

**Fig. 4: Plots of normal load versus indentation depth during the CMC indentation mode of (a) W-Cu-Ni 75-24-1, and (b) W-Cu 75-25 sintered contact materials**

In the IIT measurements, we used the quadratic loading with CMC indentation mode to obtain uniformly spaced hardness and elastic modulus values in depth. Therefore, a linear indentation depth increase was maintained in contrast with the linear loading mode where the depth increase obeys a square root curve.

During the CMC procedure consisting of repeated loading and partial unloading, the mechanical properties of W-Cu sintered contact materials were acquired from each partial unloading since the Berkovich indenter remained in contact with the tested sample.

Fig. 4 illustrates the plots of normal load versus indentation depth during the CMC indentation (20 cycles) of W-Cu sintered materials. In each cycle, the unloading was performed to 20% of the maximum load in the given cycle. Accordingly, each unload yielded discrete values of hardness and elastic modulus. Consequently, the depth profiles of indentation hardness ( $H_{IT}$ ) and elastic modulus ( $E_{IT}$ ) (Fig. 5) were achieved, along with the depth profiles of HV and HM hardness (Fig. 6).

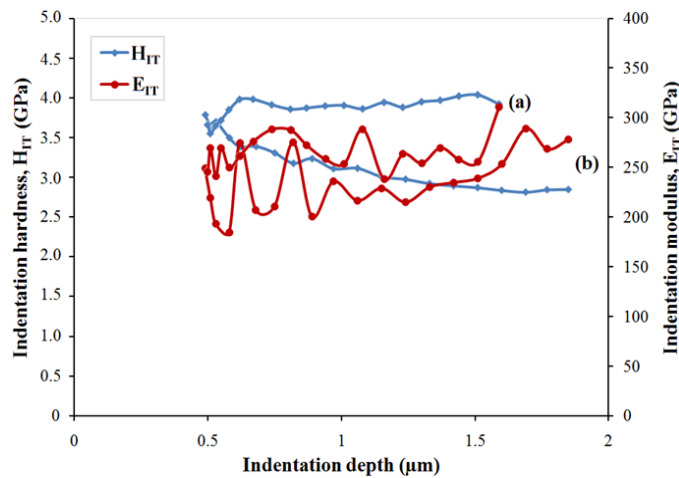


Fig. 5: Depth profiles of indentation hardness ( $H_{IT}$ ) and elastic modulus ( $E_{IT}$ ) of (a) W-Cu-Ni 75-24-1, and (b) W-Cu 75-25 sintered contact materials

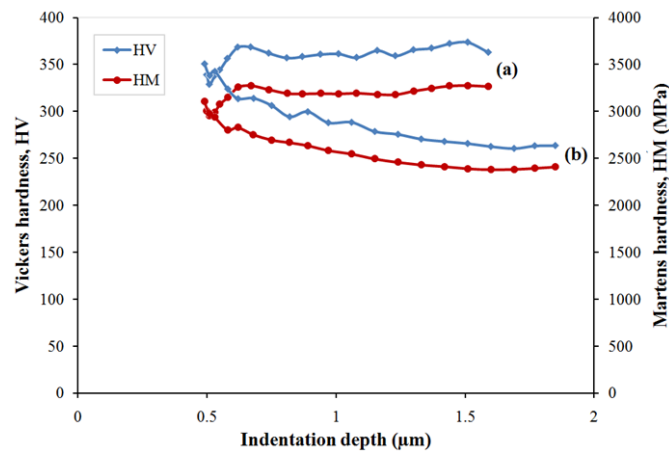


Fig. 6: Depth profiles of Vickers hardness (HV) and Martens hardness (HM) of (a) W-Cu-Ni 75-24-1, and (b) W-Cu 75-25 sintered contact materials

The mean values and standard deviation (SD) of hardness ( $H_{IT}$  and HV), indentation elastic modulus ( $E_{IT}$ ) and indentation creep ( $C_{IT}$ ) of W-Cu sintered contact materials determined by IIT measurements

and Oliver & Pharr method are summarized in Table 5. The depth profiles of indentation creep ( $C_{IT}$ ) of W-Cu sintered materials are depicted in Fig. 7

**Table 5: Mean values and standard deviation (SD) of hardness (HIT, HV), elastic modulus (EIT) and indentation creep (CIT) of the samples determined by IIT and Oliver & Pharr method**

Sintered contact material	Mean $H_{IT} \pm SD$ (GPa)	Mean HV $\pm SD$	Mean $E_{IT} \pm SD$ (GPa)	Mean $C_{IT} \pm SD$ (%)
W-Cu-Ni 75-24-1	$3.870 \pm 0.119$	$358 \pm 11$	$266 \pm 18$	$2.1 \pm 0.4$
W-Cu 75-25	$3.168 \pm 0.278$	$293 \pm 26$	$235 \pm 30$	$2.5 \pm 0.3$

The mean values of Martens hardness (HM)  $\pm SD$  of W-Cu-Ni 75-24-1 sintered contact material were

$3.177 \pm 0.089$  GPa while for W-Cu 75-25 sintered contact material were  $2.616 \pm 0.192$  GPa.

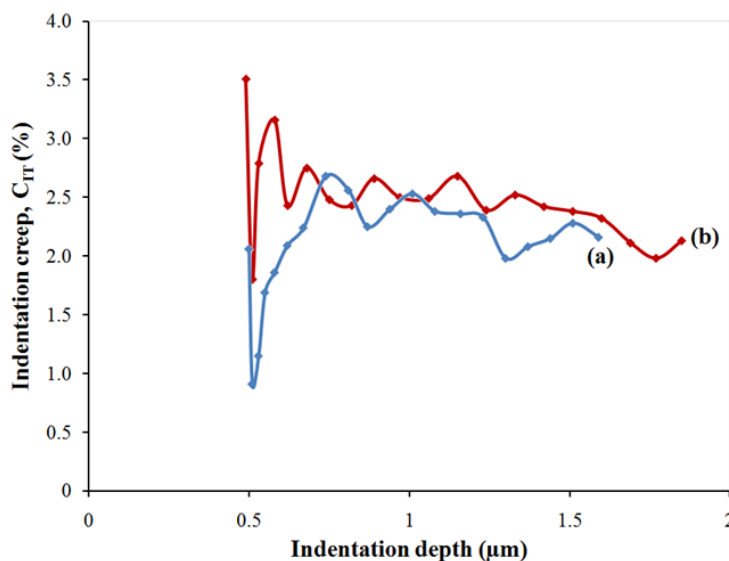
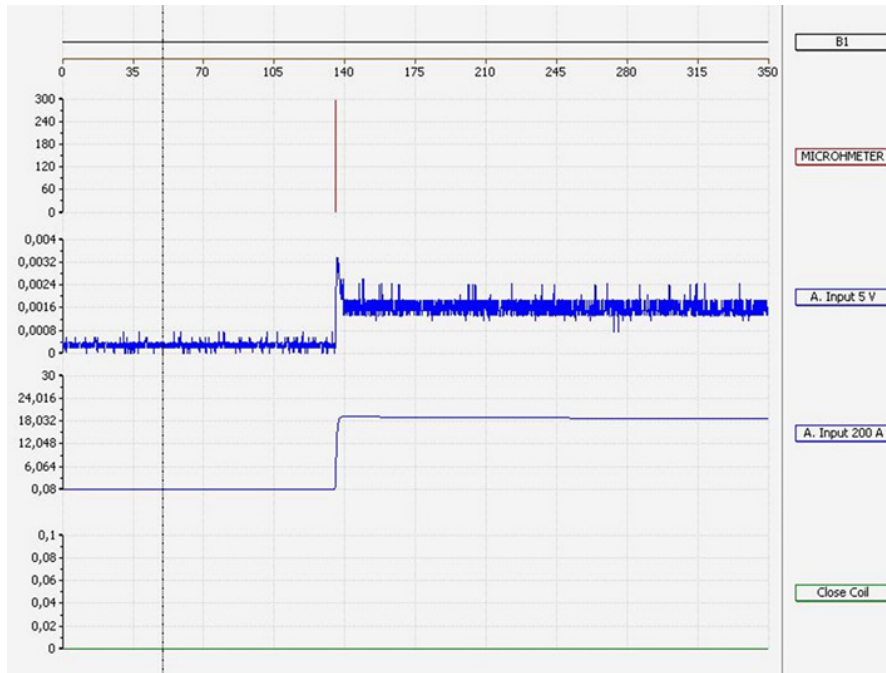


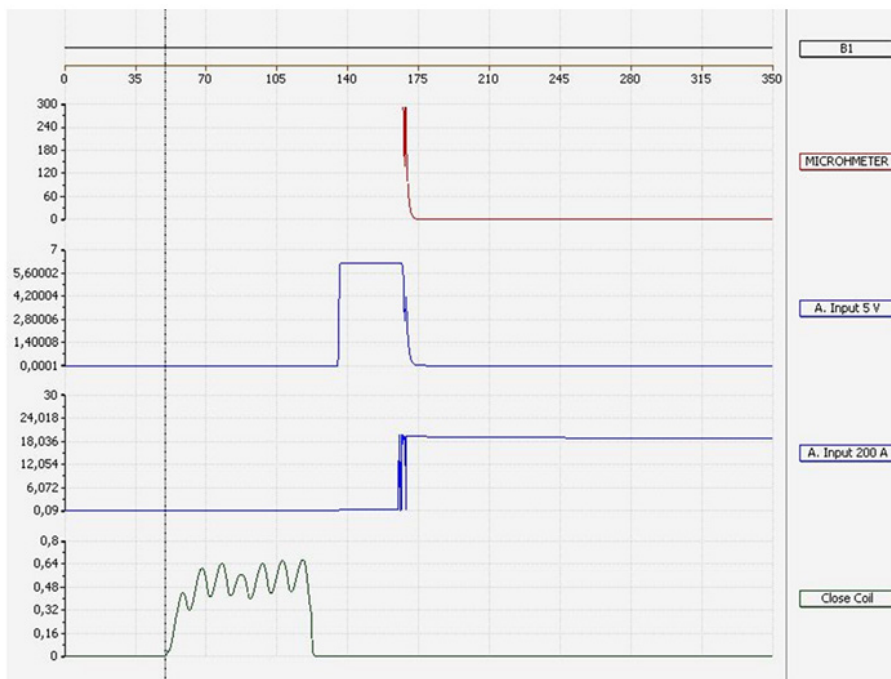
**Fig. 7: Depth profiles of indentation creep (CIT) of (a) W-Cu-Ni 75-24-1, and (b) W-Cu 75-25 sintered contact materials**

**Table 6: Mean values of static resistance (Rs), and time to reach Rs/dynamic resistance (T/Rd) of W-Cu arcing contacts**

Sintered contact material	Static contact resistance (Rs) (mΩ)	Time / Dynamic contact resistance (T/Rd) (ms/mΩ)
W-Cu-Ni 75-24-1	0.11	2 / 0.13
W-Cu 75-25	0.08	2 / 0.08

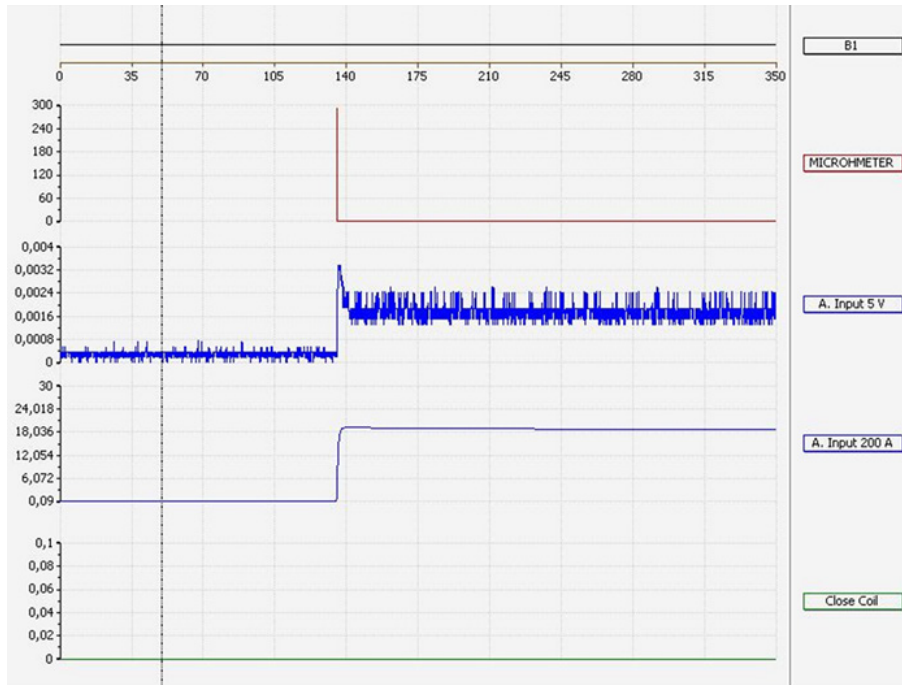


(a)

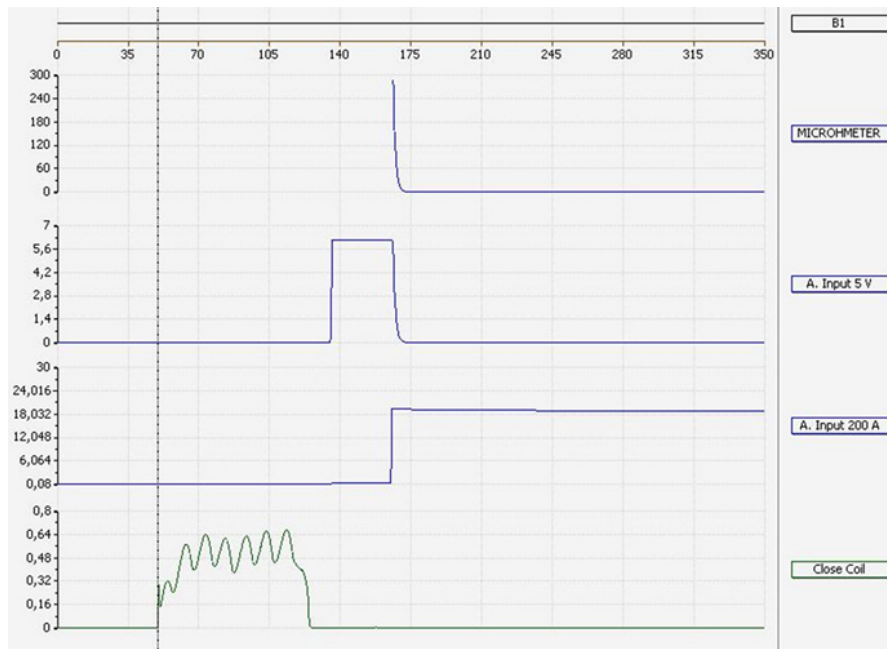


(b)

**Fig. 8:** Graphs recorded for the measurements of (a) static contact resistance ( $R_s$ ), and dynamic contact resistance ( $T/R_d$ ) of W-Cu-Ni 75-24-1 arcing contacts



(a)



(b)

**Fig. 9: Graphs recorded for the measurements of (a) static contact resistance ( $R_s$ ), and dynamic contact resistance ( $T/R_d$ ) of W-Cu 75-25 arcing contact**

The maximum indentation load ( $F_{max}$ ) of 200 mN reached the maximum indentation depth ( $h_{max}$ ) at 1.59  $\mu\text{m}$  for W-Cu-Ni 75-24-1 sintered material whereas  $h_{max}$  at  $F_{max}$  was 1.85  $\mu\text{m}$  for W-Cu 75-25 sintered material. The shallower indentation depth of W-Cu-Ni 75-24-1 material indicated higher hardness than W-Cu 75-25 material. It was noticed also that all the values of hardness (HIT, HV, and HM) increased with the decrease of  $h_{max}$  at  $F_{max}$  (Fig. 5, Fig. 6, and Table 5). Moreover, the depth profiles of hardness ( $H_{IT}$ , HV, and HM) and elastic modulus ( $E_{IT}$ ) showed a gradient in the mechanical properties of Ni doped and undoped W-Cu sintered contact materials. However, the hardness of W-Cu-Ni 75-24-1 materials varied in a lower range than W-Cu contact materials without Ni addition. It is the result of the presence of Ni and lower Cu content in W-Cu-Ni 75-24-1 sintered materials that contributed to the increase of hardness and resistance to plastic deformation while creep resistance was decreased (Fig. 7). The HV values measured in this study are in agreement with other results published in the literature.<sup>20, 29</sup> Ardestani *et al.*,<sup>20</sup> obtained HV values of about 190-310 for W-Cu contact materials with 20-40 wt.% Cu, whereas Ibrahim *et al.*,<sup>29</sup> obtained HV values of about 155-306 for W-Cu contact materials with 13-27 wt.% Cu.

The static contact resistance ( $R_s$ ) of W-Cu-Ni 75-24-1 arcing contacts at the end of the cycle, after 200 ms from the "Start" of the test was 0.11 m $\Omega$ . Moreover, the static contact resistance was constant and much lower than the maximum admissible limit of 0.2 m $\Omega$  specified in the standard IEC 62271-100. The variation of the static contact resistance with the current increase during 200 ms was lower than 0.001 m $\Omega$  (Fig. 8, a). Regarding the dynamic contact resistance (Rd) testing, the contact resistance at the end of the cycle, after 150 ms from the "Start" was 0.13 m $\Omega$ . The variation of the contact resistance from the time T4 to T8 (140 ms) was linear and constant. The variation of the resistance to contact making was oscillatory with a large slope, since the time duration from T1 to T4 was 10 ms (Fig. 8, b). The resistance Rd of 0.11 m $\Omega$  was lower than the admissible limit (0.2 m $\Omega$ ) after contact making. It was revealed also a good electrical behavior when breaking the electric arc. No microcracks in W-Cu-Ni 75-24-1 contact materials were visible after  $R_s$  and Rd testing.

W-Cu 75-25 arcing contacts had similar functional behavior as W-Cu-Ni 75-24-1 arcing contacts. The static contact resistance ( $R_s$ ) at the end of the cycle, after 200 ms from the "Start" of the test was 0.08 m $\Omega$ , which is much lower than the maximum admissible limit of 0.2 m $\Omega$ . The variation of the resistance  $R_s$  with the current increase during 200 ms was also lower than 0.001 m $\Omega$  (Fig. 9, a). Regarding the dynamic contact resistance (Rd) testing, the contact resistance at the end of the cycle, at the time T8, after 150 ms from "Start" was 0.08 m $\Omega$ . The variation of the contact resistance from the time T4 to T8 (140 ms) was linear. The variation of the resistance to contact making was exponential with a large slope, since the time duration from T1 to T4 was 10 ms (Fig. 9, b). The resistance Rd of 0.08 m $\Omega$  was lower than the admissible limit (0.2 m $\Omega$ ) after contact making. No microcracks in W-Cu 75-25 contact materials were visible after  $R_s$  and Rd testing. Conversely, superficial wear and tear of the contact material occurred at the electric arc formation.

### Conclusions

Ni doped and undoped W-Cu sintered contact materials were manufactured successfully by pressing, sintering, and liquid infiltration route.

The developed W-Cu 75-25 sintered contact materials yielded better densification, and electrical and thermal properties comparatively with W-Cu-Ni 75-24-1 sintered contact materials. However, Ni doped W-Cu exhibited better mechanical properties than undoped W-Cu sintered materials due to the addition of Ni as a sintering activator.

Ni doped and undoped W-Cu sintered contact materials exhibited good electrical behavior in terms of both  $R_s$  and Rd contact resistances since their values ranging 0.08-0.13 m $\Omega$  were lower than the admissible limit of 0.2 m $\Omega$ . Additionally, W-Cu-Ni 75-24-1 materials yielded a better electrical behavior than W-Cu 75-25 materials at breaking electric arc during operation in oil HVCBs of 110 kV.

The obtained results endorse the sintered composite materials to be used as Key Enabling Technologies (KETs) based products like arcing contacts for electric power applications, specifically in minimum oil HVCBs.

### Acknowledgments

The work was carried out under contract POC no. 133 D6 MAIRA/2019 within the Competitivity Operational Program (POC), co-funded by the European Union through the European Regional Development Fund (ERDF) program, as well as contract no. 30 PFE/2018 between the National Institute for Research and Development in Electrical Engineering ICPE-CA and the Ministry of Research and Innovation, Romania.

### Funding

The financial support to perform this study was provided by the National Authority for Scientific

Research and Innovation, Romania, and the Ministry of European Funds, Romania, through contract POC no. 133 D6 MAIRA/2019. Also, the authors acknowledge the financial support of the Ministry of Research and Innovation, Romania, through contract no. 30 PFE/2018. The funding bodies had no role in study design, data collection, analysis and interpretation, manuscript writing, and decision to submit the study for publication.

### Conflict of Interest

The authors declare that there is no potential conflict of interests regarding the publication of this article.

### References

1. M.V. Lungu, Synthesis and processing techniques of tungsten copper composite powders for electrical contact materials (A Review). *Orient. J. Chem.* 35(2), 491-515 (2019).
2. V. Tsakiris, M. Lungu, E. Enescu, D. Pavelescu, G. Dumitrescu, A. Radulian, V. Braic, W-Cu composite materials for electrical contacts used in vacuum contactors. *J. Optoelectron. Adv. M.*, 15(9-10), 1090-1094 (2013).
3. M. Lungu, V. Tsakiris, E. Enescu, D. Pătroi, V. Marinescu, D. Tălpeanu, D. Pavelescu, G. Dumitrescu, A. Radulian, Development of W-Cu-Ni electrical contact materials with enhanced mechanical properties by spark plasma sintering process. *Acta Phys. Pol. A*, 125(2), 327-330 (2014).
4. V. Tsakiris, M. Lungu, E. Enescu, D. Pavelescu, G. Dumitrescu, A. Radulian, N. Mocioi, Nanostructured W-Cu electrical contact materials processed by hot isostatic pressing. *Acta Phys. Pol. A*, 125(2), 348-352 (2014).
5. L.L. Dong, M. Ahangarkanib, W.G. Chenc, Y.S. Zhang, Recent progress in development of tungsten-copper composites: Fabrication, modification and applications. *Int. J. Refract. Met. Hard Mater.* 75, 30-42 (2018).
6. M.V. Lungu, M. Lucaci, V. Tsakiris, A. Brătulescu, C.D. Cîrstea, M. Marin, D. Pătroi, S. Mitrea, V. Marinescu, F. Grigore, D. Tălpeanu, N. Stancu, P. Godeanu, C. Melnic, Development and investigation of tungsten copper sintered parts for using in medium and high voltage switching devices. *IOP Conf. Series: Mater. Sci. Eng.* 209, 012012 (2017).
7. Q. Chen, S. Liang, F. Wang, L. Zhuo, Microstructural investigation after vacuum electrical breakdown of the W-30 wt.% Cu contact material. *Vacuum*, 149, 256-261 (2018).
8. E. Nasrallah, F. Brikci, S. Perron, Make/break contacts - in power circuit breakers. *Electric Energy (EE) T&D Magazine*, 11(3), 54 (2007).
9. C. Hou, X. Song, F. Tang, Y. Li, L. Cao, J. Wang, Z. Nie, W-Cu composites with submicron- and nanostructures: progress and challenges. *NPG Asia Mater.* 11, 74 (2019).
10. R.M. German, P. Suri, S.J. Park, Review: liquid phase sintering. *J. Mater. Sci.*, 44, 1-39 (2009).
11. Y. Zhou, Q.X. Sun, R. Liu, X.P. Wang, C.S. Liu, Q.F. Fang, Microstructure and properties of fine grained W-15 wt.% Cu composite sintered by microwave from the sol-gel prepared powders, *J. Alloys Compd.* 547, 18-22 (2013).
12. M. Ardestani, H. Arabi, H.R. Rezaie, H. Razavizadeh, Synthesis and densification of W-30% wtCu composite powders using ammonium meta tungstate and copper nitrate as precursors. *Int. J. Refract. Met. Hard Mater.* 27, 796-800 (2009).
13. S.H. Hong, B.K. Kim, Z.A. Munir, Synthesis and consolidation of nanostructured W-10-

- 40 wt.% Cu powders. *Mater. Sci. Eng. A* 405, 325-332 (2005).
14. L. Wang, L. Xu, C. Srinivasakannan, S. Koppala, Z. Han, H. Xia, Electroless copper plating of tungsten powders and preparation of WCu20 composites by microwave sintering. *J. Alloys Compd.* 764, 177-185 (2018).
  15. L. Xu, M. Yan, J. Peng, C. Srinivasakannan, Y. Xia, L. Zhang, G. Chen, H. Xia, S. Wang, Influences of temperatures on tungsten copper alloy prepared by microwave sintering. *J. Alloy. Compd.* 611, 34-37 (2014).
  16. L. Xu, C. Srinivasakannan, L. Zhang, M. Yan, J. Peng, H. Xia, S. Guo, Fabrication of tungsten-copper alloys by microwave hot pressing sintering. *J. Alloy. Compd.* 658, 23-28 (2016).
  17. L. Xu, M. Yan, Y. Xia, J. Peng, W. Li, L. Zhang, C. Liu, G. Chen, Y. Li, Influence of copper content on the property of Cu-W alloy prepared by microwave vacuum infiltration sintering. *J. Alloy. Compd.*, 592, 202-206 (2014).
  18. A. Mondal, A. Upadhyaya, D. Agrawal, Effect of heating mode and copper content on the densification of W-Cu Alloys, *Indian J. Mater. Sci.* 2013, 603791 (2013).
  19. G.T.P. Azar, H.R. Rezaie, H. Razavizadeh, Synthesis and consolidation of W-Cu composite powders with silver addition. *Int. J. Refract. Met. Hard Mater.* 31, 157-163 (2012).
  20. M. Ardestani, H.R. Rezaie, H. Arabi, H. Razavizadeh, The effect of sintering temperature on densification of nanoscale dispersed W-20-40%wt Cu composite powders. *Int. J. Refract. Met. Hard Mater.* 27, 862-867 (2009).
  21. M. Hashempour, H. Razavizadeh, H.R. Rezaie, M.T. Salehi, Thermochemical preparation of W-25%Cu nanocomposite powder through a CVT mechanism. *Mater. Charact.* 60, 1232-1240 (2009).
  22. M. Hashempour, H.R. Rezaie, H. Razavizadeh, M.T. Salehi, H. Mehrjoo, M. Ardestani, Investigation on fabrication of W-Cu nanocomposite via a thermochemical co-precipitation method and its consolidation behavior. *J. Nano Res.* 11, 57-66 (2010).
  23. J. Cheng, C. Lei, E. Xiong, Y. Jiang, Y. Xia, Preparation and characterization of W-Cu nanopowders by a homogeneous precipitation process. *J. Alloys Compd.* 421, 146-150 (2006).
  24. A. Chu, Z. Wang, D. Rafiud, Y. Dong, C. Guo, W. Liu, H. Xu, L. Wang, Citric acid-assisted combustion-nitridation-denitridation synthesis of well-distributed W-Cu nanocomposite powders. *Int. J. Refract. Met. Hard Mater.* 70, 232-238 (2018).
  25. D. Ma, J. Xie, J. Li, A. Wang, W. Wang, Contact resistance and arc erosion of tungsten-copper contacts in direct currents. *J. Wuhan Univ. Technol. – Mater. Sci.* 32 (4), 816-822 (2017).
  26. W.C. Oliver, G.M. Pharr, An improved technique for determining hardness and elastic modulus using load and displacement sensing indentation experiments. *J. Mater. Res.* 7(6), 1564-1583 (1992).
  27. S. Zinelis, Y.S. Al Jabbari, M. Gaintantzopoulou, G. Eliades, T. Eliades, Mechanical properties of orthodontic wires derived by instrumented indentation testing (IIT) according to ISO 14577. *Prog. Orthod.* 16(1), 19 (2015).
  28. K. Zangeneh-Madar, M. Amirjan, N. Parvin, Improvement of physical properties of Cu-infiltrated W compacts via electroless nickel plating of primary tungsten powder. *Surf. Coat. Technol.* 203, 2333-2336 (2009).
  29. H. Ibrahim, A. Aziz, A. Rahmat, Enhanced liquid-phase sintering of W-Cu composites by liquid infiltration. *Int. J. Refract. Met. Hard Mater.* 43, 222-226 (2014).
  30. S. Borji, M. Ahangarkani, K. Zangeneh-Madar, Z. Valefi, The effect of sintering activator on the erosion behavior of infiltrated W-10wt% Cu composite. *Int. J. Refract. Met. Hard Mater.* 66, 150-157 (2017).
  31. Anton Paar GmbH. (2020, January 14). A Guide to Anton Paar Indentation Modes. AZoM. Retrieved on May 5, 2020 from <https://www.azom.com/article.aspx?ArticleID=13980>